International Journal of Advances in Data and Information Systems
Vol. 6, No. 2, August 2025, pp. 308~319
ISSN: 2721-3056, DOI: 10.59395/ijadis.v6i2.1388

Integrating Satellite Imagery and Multicriteria Decision Analysis for High-Resolution Flood Vulnerability Mapping: A Case Study of Jakarta, Indonesia

Atut Pindarwati[1], Arie Wahyu Wijayanto[2], Perani Rosyani[1], Meilinda F. N. Maghfiroh[3]
[1]Department of Computer Science, Pamulang University, Indonesia
[2]Department of Statistical Computing, Politeknik Statistika STIS, Indonesia
[3]Faculty of Transport and Logistics, Muscat University, Al Ghubra North, Muscat, Sultanate of Oman

Article Info

Article history:

Received May 08, 2025
Revised May 28, 2025
Accepted Jul 12, 2025

Keywords:

Satellite Imagery, Analytic Hierarchy Process, Flood Vulnerability, Multi-Criteria Decision Analysis

ABSTRACT

Jakarta, Indonesia, ranks among the most flood-prone megacities in the world, with hydrometeorological factors placing up to 98% of its area at flood risk. Its population density—approximately 15,900 individuals per square kilometer—compounds the impacts of flooding through intensified exposure and socio-economic vulnerability. This study presents a novel, data-driven methodology for flood vulnerability assessment in the Jakarta Special Capital Region (DKI Jakarta), integrating satellite remote sensing and geospatial analysis with a Multicriteria Decision Analysis (MCDA) framework. Employing the Analytical Hierarchy Process (AHP) to systematically weight environmental and socio-economic criteria, a Flood Vulnerability Index (FVI) was developed and spatially modeled at a 500-meter grid resolution. The resulting FVI map categorizes vulnerability into five levels: very low, low, moderate, high, and very high. Findings indicate an index range between 0.36 and 0.70, highlighting predominantly moderate to high vulnerability zones across the region. This high-resolution assessment provides actionable insights for disaster risk reduction, urban resilience planning, and targeted policy interventions to mitigate flood-related hazards in Jakarta.

This is an open access article under the CC BY-SA license.

Corresponding Author:

Arie Wahyu Wijayanto,
Department of Statistical Computing,
Politeknik Statistika STIS,
Jakarta, Indonesia.
Email: ariewahyu@stis.ac.id

1. INTRODUCTION

Vulnerability to disasters represents the susceptibility of communities and environments to disruption, resulting in losses due to specific disasters [1]. Floods are among the disasters that require vigilant attention. A flood occurs when normally dry areas are inundated with water due to saturated soil drainage levels and maximum water infiltration capacity. The flood vulnerability index serves as a more specific instrument in measuring the losses caused by disasters, particularly floods. The study focuses on the Jakarta Special Capital Region, which covers 662 km² of land and 6,977 km² of sea, characterized by flat terrain with an average elevation of 7 meters above sea level, with 40% of the area, especially the northern part, lying below sea level [2]. Jakarta is also known as "The Big Durian" because it is considered a city comparable to New York City (Big Apple) in the United States [3]. The region is intersected by rivers flowing from the Jonggol and

Puncak areas, with the Ciliwung River dividing the city into west and east. According to National Agency for Disaster Countermeasure (BNPB) data, Jakarta faces a 98% potential flood risk due to hydrometeorological factors. With a dense population of approximately 15,900 people per km², Jakarta is the ninth most populous city globally, exacerbating the flood disaster risk due to complex socio-economic issues.

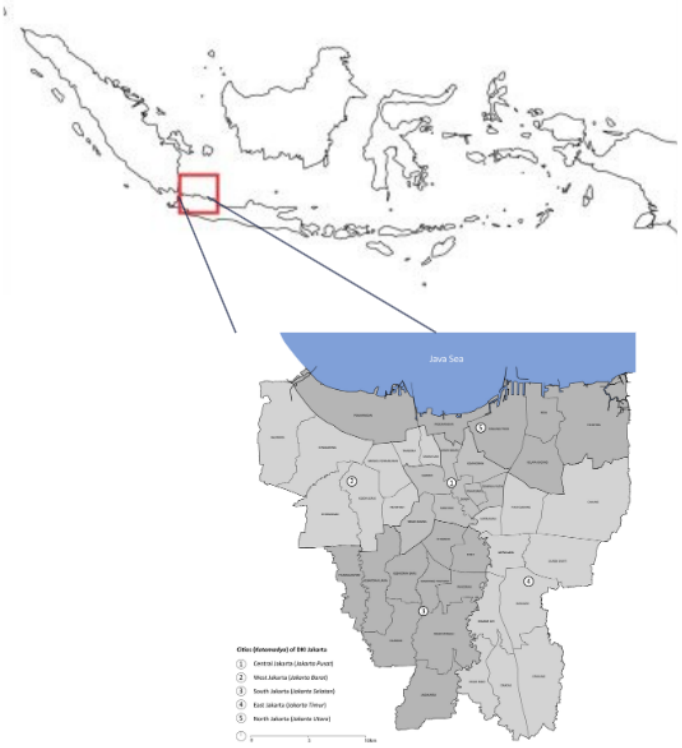


Figure. 1. Jakarta as a research study

This study constructs an estimation index of flood vulnerability using the Multicriteria Decision Analysis (MCDA) method with satellite image data. The study aims to develop an automated index to assess flood vulnerability potential, particularly in the Jakarta Special Capital Region, utilizing Sentinel-2 satellite imagery and The United States National Aeronautics and Space Administration (NASA) Shuttle Radar Topography Mission (SRTM) data. The second approach employs the Analytical Hierarchy Process (AHP) within the framework of Multiple Criteria Decision Analysis (MCDA) to build an estimation index of vulnerability to floods. This index utilizes several indicators obtained through satellite image analysis and geospatial data. The geospatial multispectral indicators of water bodies, vegetation, and building density will be extracted from Sentinel-2 satellite imagery, while Elevation and Slope data will be obtained from NASA Shuttle Radar Topography Mission (SRTM) satellite imagery. Additionally, satellite image data and geospatial analysis will be acquired through the Google Earth Engine (GEE) platform.

Once the indices have been constructed, evaluation will be conducted by measuring various performance metrics. In the AHP method, the evaluation will involve calculating the Consistency Ratio (CR) to ensure that the results of the multicriteria decision analysis are consistent. CR is a metric used to evaluate the consistency of pairwise comparisons in AHP.

The results of this evaluation will help assess the quality and validity of both approaches used in this study, ensuring that the results are reliable and useful in the context of flood vulnerability estimation. The study categorizes flood vulnerability into four classes: very low (0-0.2), low (0.2-0.4), moderate (0.4-0.6), high (0.6-0.8), and very high (0.8-1). The results manifest as a map with a 500-meter * 500-meter grid resolution, revealing a vulnerability index range of 0.36 - 0.70 for DKI Jakarta. A comparison with the district-level map shows a range of 0.460568 - 0.636578, while at the village level, the range is 0.437806 - 0.648402. DKI Jakarta falls within the moderate to high vulnerability levels.

While supervised machine learning and traditional regression models can be powerful for pattern recognition, they required labeled data of the area-level flood vulnerability. In contrast, AHP allows structured integration of expert knowledge and accommodates both quantitative and qualitative criteria. In Jakarta case, official area-level flood vulnerability up to grid level is not available compared to the existing administrative level data. Hence, MCDA is more suitable approach.

This study presents a novel integration of high-resolution satellite imagery and Multicriteria Decision Analysis (MCDA) using the Analytical Hierarchy Process (AHP) to generate a detailed Flood Vulnerability Index (FVI) for Jakarta, Indonesia. By implementing a 500-meter grid resolution, the resulting vulnerability map effectively classifies urban areas into five distinct categories—very low to very high vulnerability. This approach enables spatially explicit identification of flood-prone zones, offering a scalable and data-driven framework for urban flood risk assessment. The resulting map provides actionable insights for policymakers and disaster risk managers, supporting targeted mitigation strategies, infrastructure planning, and resilience-building efforts in one of the world's most flood-affected megacities.

2. RESEARCH METHOD

This section explains the materials used in the research and the types of equipment used. There are also explanations about the steps of solving the problem.

2.1 Data Used

In this study, several indicators were used, divided into five categories: Building Density, Vegetation Density, Water Bodies, Slope, and Elevation. For Building Density, two indices were used: the Built-Up Index (BUI) to detect the level of built-up land considering vegetation effects, and the Normalized Difference Built-Up Index (NDBI) to detect the level of built-up land. Then, for Vegetation Density, two indices were used: the Soil Adjusted Vegetation Index (SAVI) to detect vegetation levels considering soil brightness factors, and the Normalized Difference Vegetation Index (NDVI) to detect vegetation levels. Additionally, the Normalized Difference Water Index (NDWI) was used to detect the level of land wetness for the Water Bodies indicator. Furthermore, indicators for Slope and Elevation were used: Slope to detect the degree of slope in an area, and Elevation to detect the elevation level of an area.

In this study, satellite imagery from Sentinel-2 was utilized to support the analysis. Sentinel-2 is equipped with the Multispectral Instrument (MSI), which captures data across 13 spectral bands with a revisit time of approximately five days (European Space Agency, n.d.). These spectral bands are acquired at varying spatial resolutions: four bands at 10 meters, six bands at 20 meters, and three bands at 60 meters. The Level-2A products used in this research originally had a spatial resolution of 10 meters (S2-10), and were resampled to 30 meters (S2-30) to ensure compatibility with other spatial datasets used in the analysis.

Table 1. Spectral Band Characteristics of Sentinel-2 MSI Level-2A

Band	Description	Spatial Resolution (m)	Central Wavelength (nm) (S2A / S2B)
B1	Aerosol	60	443.9 / 442.3
B2	Blue	10	490.0 / 492.4
B3	Green	10	560.0 / 559.8
B4	Red	10	665.0 / 664.6
B5	Red Edge 1	20	705.0 / 703.9
B6	Red Edge 2	20	740.0 / 739.1
B7	Red Edge 3	20	783.0 / 779.7
B8	Near-Infrared (NIR)	10	842.0 / 832.9
B8A	Red Edge 4	20	865.0 / 864.0
B9	Water Vapor	60	945.0 / 943.2
B10	Cirrus	60	1375.0 / 1376.9
B11	Shortwave IR 1	20	1610.0 / 1613.7
B12	Shortwave IR 2	20	2190.0 / 2202.4

The BUI, NDBI, SAVI, NDVI, and NDWI indicators were obtained from Sentinel-2 satellite imagery, while the slope and elevation indicators were obtained from NASA-SRTM satellite imagery with a data collection period from January 1, 2023, to December 31, 2023. The raster data collection was conducted by covering the study area, which is the entire area of DKI Jakarta Province, using polygons with a 500-meter * 500-meter grid performed with Google Earth Engine software. Raster data from Sentinel-2 were processed according to the formulation of each raster-forming band as displayed in Table 1. Subsequently, all obtained raster results were further processed using the Quantum-GIS (QGIS) application. Although Sentinel-2 provides 10–30m resolution, a 500m grid was chosen to align with urban management scales and reduce computational load, especially for zonal statistics and regional policy planning. While this may smooth finer details, it enables practical application at the city-wide level.

Table 1. The Indicators and Data Source

No.	Indicator Category	Index Parameters Utilized	Bands Utilized	References	Source Data	Spatial Resolution
1.	Building Density	*Built-Up Index* (BUI)	B4 (Red), B8 (NIR), and B11 (SWIR 1)	Kaimaris & Patias, 2016	Sentinel-2	10m
2.		*Normalized Difference Built-Up Index* (NDBI)	B8 (NIR) and B11 (SWIR 1)	Saadi&Wijayanto, 2021		
3.	Vegetation Density	*Soil Adjusted Vegetation Index* (SAVI)	B4 (Red) and B8 (NIR)	Zhen et al, 2021		
4.		*Normalized Difference Vegetation Index* (NDVI)	B2 (Blue), B4 (Red), and B8 (NIR)	Huang et al, 2021		
5.	Water Bodies	*Normalized Difference Water Index* (NDWI)	B8 (NIR) and B3 (Green)	McFeeter, 1996)		
6.	Slope	Slope	Slope	Aryal et al, 2020	NASA-SRTM	30m
7.	Elevation	Elevation	Elevation	Bhuiyan et al, 2014		

Next, based on the information provided in Table 1 above, we will present detailed information for each indicator along with the formulas used to calculate the value per indicator, including BUI, NDBI, NDVI, SAVI, NDWI, slope, and elevation. These details are expected to provide a deeper understanding of each parameter used in this analysis, as follows:

a) Built-Up Index (BUI)

The Built-Up Index (BUI) is essentially similar to NDBI, which is used to detect built-up areas in a region. However, BUI is superior to NDBI because it eliminates the vegetation component (NDVI) in its formulation (Kaimaris & Patias, 2016). Thus, BUI is considered more precise in identifying the level of built-up land in an area, but the use of NDBI cannot be disregarded entirely as they complement each other for specific conditions. In its calculation, BUI the following formula.

$$\mathrm{BUI} = \mathrm{NDBI} - \mathrm{NDVI} \quad (1)$$

Where,

BUI : *Built-Up Index*

$NDBI$: *Normalized Difference Built-Up Index*

$NDVI$: *Normalized Difference Vegetation Index*

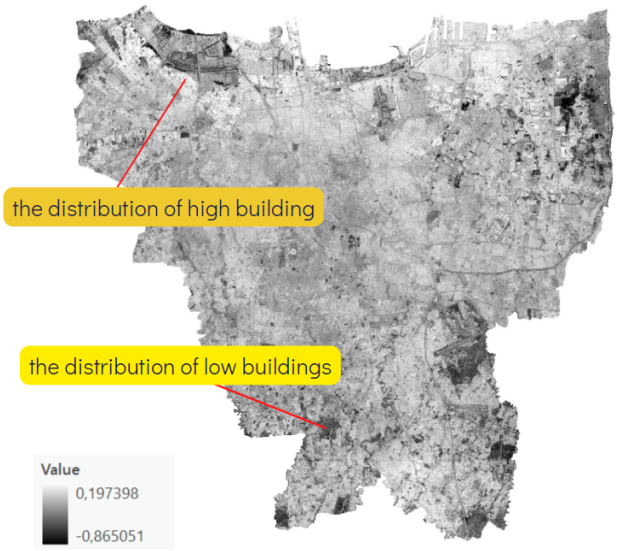


Figure 2. Visualization Map of *Built-Up Index* (BUI) Jakarta

b) Normalized Difference Built-Up Index (NDBI)

The Normalized Difference Built-Up Index (NDBI) is an index used to depict the extent of built-up areas in a region. The classification range of NDBI values is between -1 and 1, where negative values represent water bodies, while higher values depict built-up areas (Saadi & Wijayanto, 2021). The calculation of NDBI can be performed using the following formula.

$$\text{NDBI} = \frac{\text{SWIR} - \text{NIR}}{\text{SWIR} + \text{NIR}} \qquad (2)$$

Where,

$NDBI$: *Normalized Difference Built-Up Index*

NIR : *Near Infrared* which involves the values of pixels from the nearest infrared band

$SWIR$: *Short Wavelength Infrared*

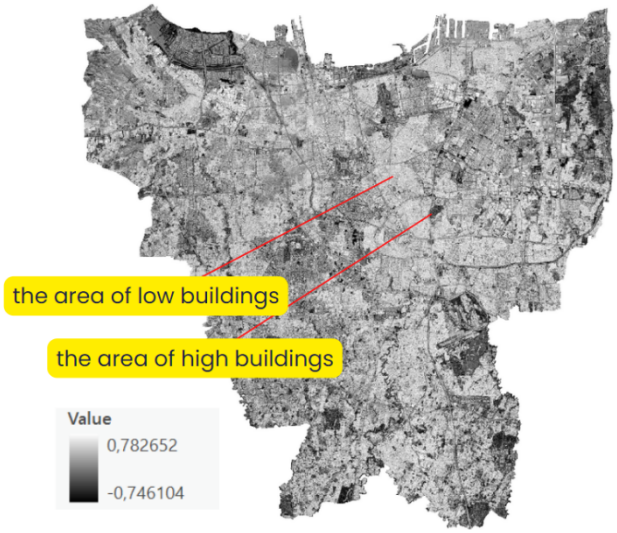


Figure 3. Visualization Map of *Normalized Difference Built-Up Index* (NDBI) Jakarta

c) Normalized Difference Vegetation Index (NDVI)

NDVI is an index used to depict the vegetation cover of an area (Huang et al., 2021). The classification range of NDVI values ranges from -1 to 1 (Aquino et al., 2018). The calculation of NDVI is performed using the following formula:

$$\text{NDVI} = \frac{\text{NIR} - \text{Red}}{\text{NIR} + \text{Red}} \quad (3)$$

Where,
NDVI : *Normalized Difference Vegetation Index*
NIR : *Near Infrared* which refers to the pixel values from the nearest infrared band.
Red: Pixel values from the nearest red band.

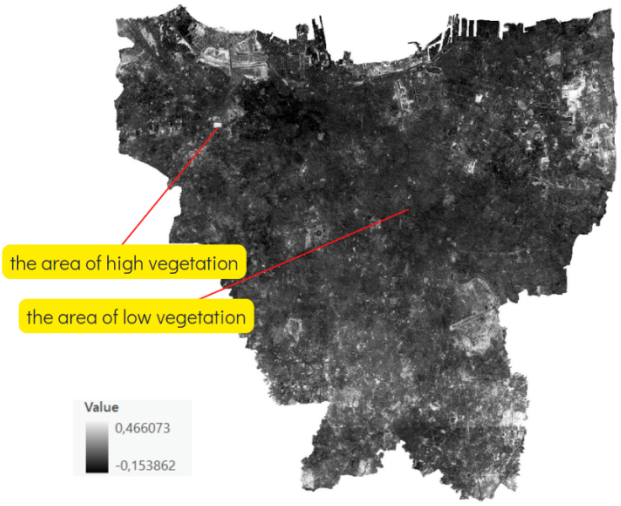


Figure 4. Visualization Map of Normalized Difference Vegetation Index (NDVI) Jakarta

d) *Soil Adjusted Vegetation Index* (SAVI)

Soil Adjusted Vegetation Index (SAVI) is an enhancement of NDVI as it serves the same function, which is to detect vegetation levels, but SAVI takes into account soil brightness factors (Zhen et al., 2021). With the following calculation formula, the classification range of SAVI values is between -1 and 1.

$$\text{SAVI} = \left(\frac{\text{NIR} - \text{Red}}{\text{NIR} + \text{Red} + \text{L}}\right)(1 + \text{L}) \quad (4)$$

Di mana,
SAVI : *Soil Adjusted Vegetation Index*
NIR : *Near Infrared* which refers to the pixel values from the nearest infrared band.
Red : Pixel values from the nearest red band
L : Total green vegetation cover

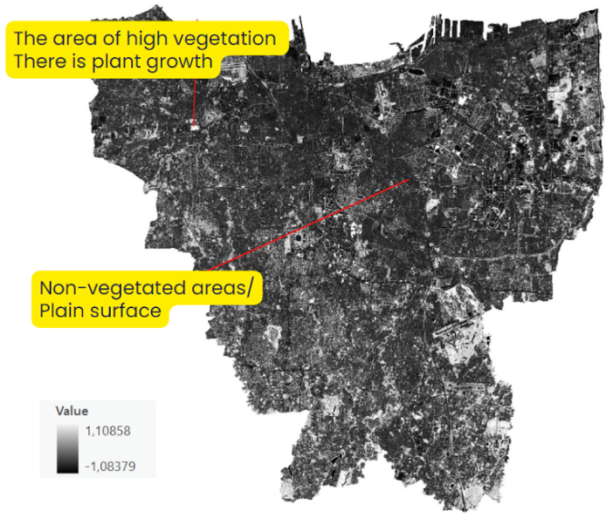


Figure 5. Visualization Map of *Soil Adjusted Vegetation Index* (SAVI) Jakarta

e) Normalized Difference Water Index (NDWI)

Normalized Difference Water Index (NDWI) is a remote sensing technique used to detect the presence of water in an area. This index is utilized to highlight open water features and enhance their presence in remote sensing imagery [8]. NDWI is calculated using the combination of GREEN-NIR (visible green and near-infrared), enabling it to detect small changes in water content in water bodies. NDWI values greater than 0.5 typically correspond to water bodies, while vegetation and built-up areas correspond to smaller values between zero and 0.5, respectively.

$$\text{NDWI} = \frac{\text{Green} - \text{NIR}}{\text{Green} + \text{NIR}} \quad (5)$$

Di mana,

NDWI : *Normalized Difference Water Index*

NIR : *Near Infrared* which refers to the pixel values from the nearest infrared band.

Green : Reflectance Band Green Color

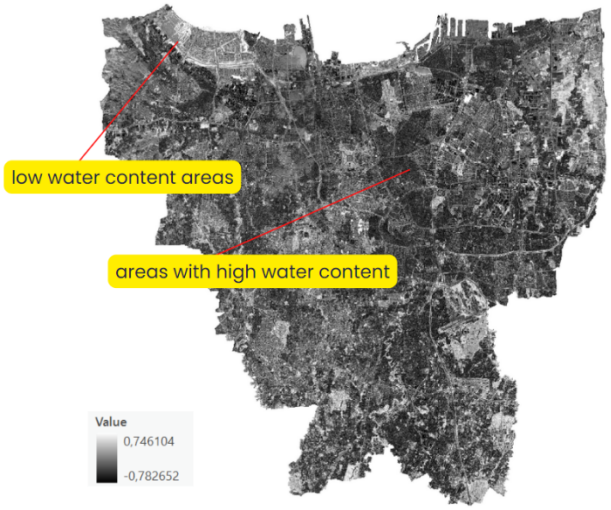


Figure 6. Visualization Map of *Normalized Difference Water Index* (*NDWI)* Jakarta

f) Slope and Elevation

Slope is obtained through Digital Elevation Model (DEM) by calculating the pixel value difference of each pixel from the maximum elevation, as well as the distance of each pixel from the maximum elevation to its four connected neighboring pixels. This process can be implemented using the Slope() function from Google Earth Engine (Aryal et al., 2020).

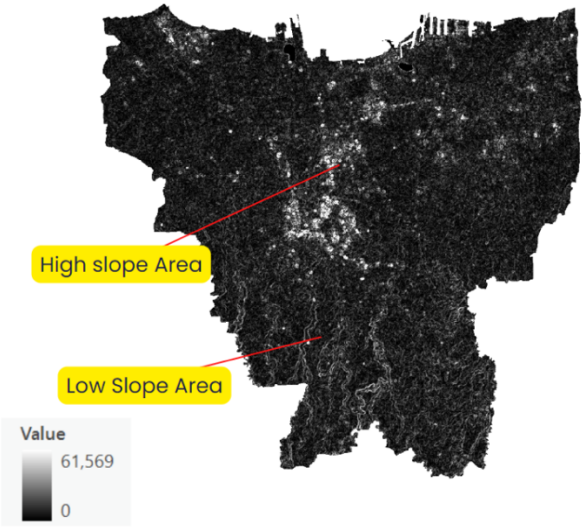


Figure 7. Visualization Map of Slope Jakarta

Elevation is information about the altitude of a location or point on the Earth's surface, obtained through a Digital Elevation Model (DEM) that maps topography with a resolution of up to 30 meters (Bhuiyan et al., 2014).

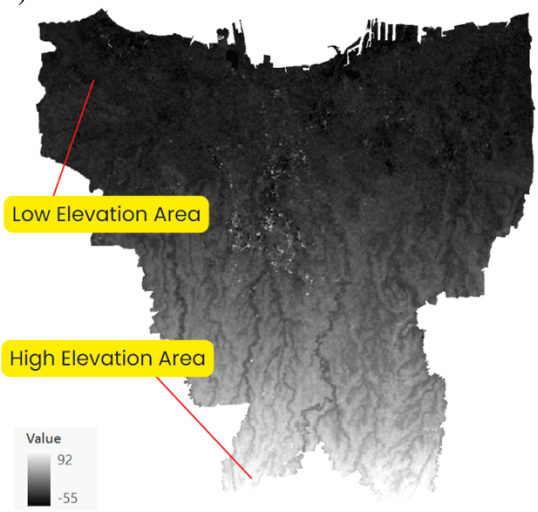


Figure 8. Visualization Map of Elevation Jakarta

2.2 Analytical Hierarchy Process (AHP) for Flood Vulnerability Index

To fulfill the objectives of this study, weight calculation will be conducted for each index category. The weights for each indicator are calculated based on the predetermined range scale. These weights will be used in the subsequent analysis to determine the level of flood The Analytical Hierarchy Process (AHP) is a structured approach used to analyze problems by assigning weights to different factors (Saaty & Katz, 1990). These weights indicate the relative importance of each factor. Importance is measured on a scale of 1 to 9, where 1 signifies low importance and 9 signifies high importance. In Table 3, alternative weights are presented to compare the contributions of various indicators (Saaty & Katz, 1990).

Table II. Weight of AHP

No	Weight	Value
1.	1	Equal Importance
2.	3	Moderate Importance
3.	5	Stronger Importance
4.	7	Very Strong Importance
5.	9	Very Important
6.	2,4,6,8	Moderately Important

The AHP pairwise comparisons were informed by expert judgment through discussion with a single domain specialist—a remote sensing analyst with expertise in disaster vulnerability assessment. This expert provided input on the relative importance of each criterion based on practical experience and thematic knowledge. The resulting pairwise comparison matrix was constructed accordingly, and its consistency was verified using the Consistency Ratio (CR), which yielded a value of 0.07, indicating acceptable consistency in the judgment process.

The zonal statistics is a spatial analysis tool used to calculate statistics from raster cell values within specific zones defined by other raster or vector datasets. The resulting statistics include mean, median, sum, standard deviation, and others. This tool is helpful in obtaining an overview of the statistical characteristics of specific zones, such as average temperature based on land use type. The results of zonal statistics are attached to all cells corresponding to specific zones, allowing for comparisons between zones and monitoring trends over time. In this study, zonal statistics calculates the mean value for each 500 m * 500 m grid using the following formula:

$$Mean = \frac{1}{n}\sum_{i=1}^{n} xi \quad (6)$$

Where

n Number of Observation
xi Observed Value

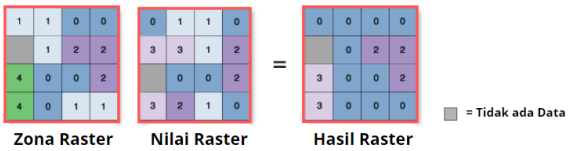


Figure 9. *Zonal Statistic*

3 RESULTS AND DISCUSSION

3.1 Flood Vulnerability Index and Mapping

The calculation of the flood vulnerability index is conducted using the weights obtained from the Analytical Hierarchy Process (AHP). The calculation is performed using the following formula:

$$LC = \frac{1}{n}\sum_{i=1}^{n} D_i W_i$$
$$= 1/7((BUI\ x\ W_{BUI}) - (SAVI\ x\ W_{SAVI}) + (NDWI\ x\ W_{NDWI}) - (Slope\ x\ W_{slope}) - (NDVI\ x\ W_{NDVI}) - (Elevation\ x\ W_{elevation}) + (NDBI\ x\ W_{NDBI})) \quad (7)$$

This calculation will then produce a flood vulnerability map that is reclassified into categories of very high, high, medium, low, and very low. This LC formula serves to connect the AHP weights and the use of geospatial data

The Global Flood Mapper (GFM) is a web application that empowers users to swiftly generate flood vulnerability maps without requiring intricate technical knowledge. It employs an algorithm that integrates Sentinel-1 data identified during floods with Z-score values and historical flood event data to map surface inundation during flood occurrences. By incorporating these elements, the algorithm effectively maps surface inundations during flood events and differentiates between water bodies and inundations caused by floods [14].

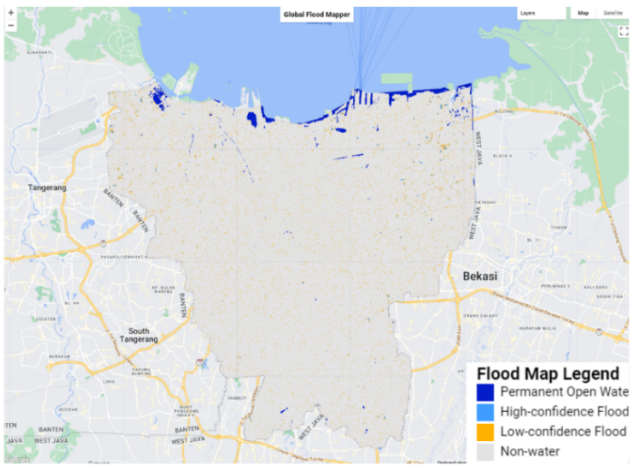


Figure 10. Jakarta's map low flood vulnerability based on the Global Flood Mapper (GFM) map

An evaluation was conducted by comparing the identification of extreme points on flood vulnerability maps generated using the AHP method with those from the Global Flood Mapper (GFM). The results revealed a significant overlap in the identified areas. This finding suggests that the AHP-based flood vulnerability mapping method can serve as an alternative tool for monitoring flood vulnerability levels in a given region.

To assess the robustness of the AHP-based weighting, a basic sensitivity test was conducted by adjusting weights ±10%. The resulting vulnerability maps showed minimal reclassification in high-risk zones, indicating moderate stability of the model. However, more rigorous sensitivity analysis is recommended for future refinement.

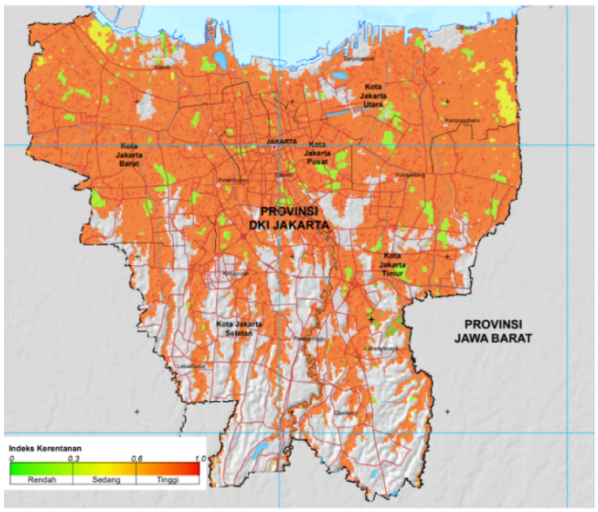


Figure 15. Flood Vulnerability Map of DKI Jakarta from Indonesia's BNPB (National Disaster Management Agency)

The National Disaster Management Agency (BNPB) leverages information sources like provincial/district cstatistics and the Village Potential Survey (PODES) gathered through conventional survey methods

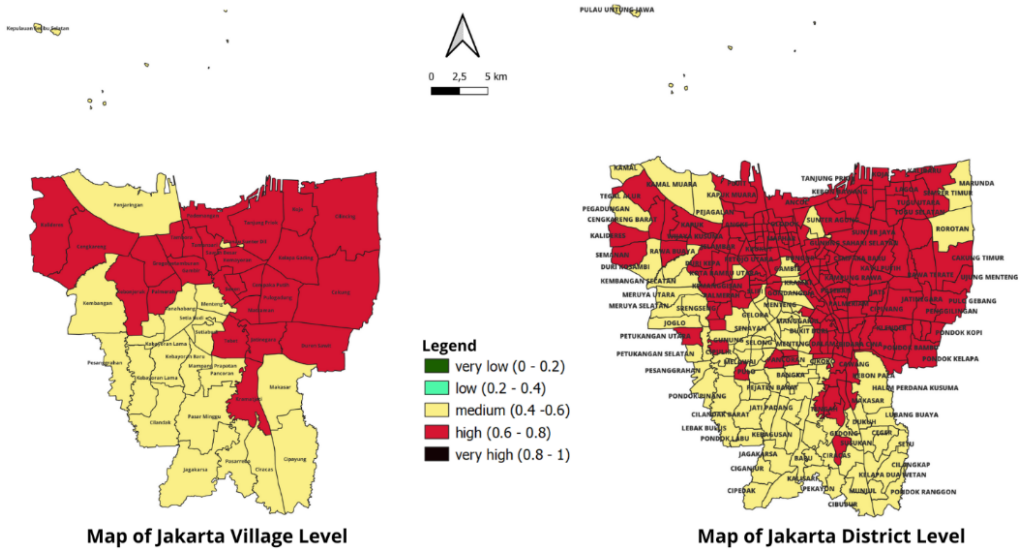


Figure 11. Map of Jakarta District Level and Village Level

3.2 Discussion

This study aims to provide a granular flood vulnerability assessment at a high spatial resolution of 500 meters, enabling localized analysis across Jakarta. However, variables such as rainfall intensity, drainage infrastructure, land use zoning, and socio-economic indicators like

household income and building materials were not incorporated due to the lack of data available at this fine spatial scale. These variables are typically aggregated at coarser administrative levels, making them unsuitable for integration into a grid-based approach. Future research is encouraged to incorporate these factors as higher-resolution datasets become accessible, thereby improving the comprehensiveness and accuracy of flood vulnerability modeling.

While visual comparison with flood-related references such as the Global Flood Monitoring (GFM) dataset and BNPB flood hazard maps supports the plausibility of the identified high-risk zones, no direct quantitative validation using historical flood extent data (e.g., the 2020 Jakarta flood) was conducted due to data access limitations. Consequently, accuracy metrics such as precision, recall, or the Kappa index were not computed.

It is also important to emphasize that flood vulnerability reflects the underlying susceptibility or probability of being affected, which is inherently different from flood incidence or actual occurrence. A location may be highly vulnerable due to terrain, land use, or exposure characteristics, even if it has not recently experienced a flood event. Therefore, direct validation against past flood footprints—while informative—does not fully capture the nature of vulnerability assessments. This remains a key area for future research, particularly with the integration of time-series flood observation data.

4 CONCLUSION

In conclusion, the study highlights the significance of utilizing remote sensing techniques for assessing flood vulnerability. By leveraging indices such as NDVI, NDBI, SAVI, NDWI, slope, and elevation derived from satellite imagery, the analysis provides valuable insights into the spatial distribution of built-up areas, vegetation cover, water bodies, and terrain characteristics, which are crucial for understanding flood-prone areas.

The evaluation of flood vulnerability, incorporating metrics such as the Consistency Ratio in AHP, ensures the reliability and validity of the results. This comprehensive approach aids in informed decision-making for disaster management and urban planning, thereby enhancing resilience against flood hazards. An automated model is developed to estimate flood vulnerability potential at a 500-meter grid resolution. The Analytical Hierarchy Process (AHP) within the MCDA framework facilitates the construction of the vulnerability index, categorized into five classes: very low, low, moderate, high, and very high. The results reveal a vulnerability index range of 0.36 - 0.70 for DKI Jakarta, indicating moderate to high vulnerability levels.

Moving forward, further research and refinement of methodologies will continue to advance flood vulnerability estimation, contributing to the development of more effective mitigation strategies and sustainable urban planning

REFERENCES

[1] X. S. Li, et al., "Analysis and Simplification of Three-Dimensional Space Vector PWM for Three-Phase Four-Leg Inverters," IEEE Transactions on Industrial Electronics, vol. 58, pp. 450–464, Feb. 2011.

[2] Y. Hirabayashi et al., "Global flood risk under climate change," Nature Climate Change, vol. 3, no. 9, pp. 816–821, 2013, doi: 10.1038/nclimate1911.

[3] United Nations Environmental Program, "How climate change is making record-breaking floods the new normal," Mar. 3, 2020. [Online]. Available: https://www.unep.org/news-and-stories/story/how-climate-change-making-record-breaking-floods-new-normal

[4] Badan Pusat Statistik Provinsi DKI Jakarta, Provinsi DKI Jakarta dalam angka 2021, p. 74, 2021. [Accessed: Apr. 11, 2024].

[5] Badan Pusat Statistik Provinsi DKI Jakarta, Jumlah penduduk menurut agama dan kabupaten/kota di Provinsi DKI Jakarta 2020, 2020. [Accessed: Apr. 15, 2024].

[6] M. Suryodiningrat, "Jakarta: A city we learn to love but never to like," The Jakarta Post, Jun. 22, 2007. [Archived: Feb. 21, 2008; Accessed: Dec. 2, 2023].

[7] J. P. Aquino, A. M. Monteiro, and J. L. Figureueiredo, "Remote sensing techniques for vegetation mapping in tropical rainforests," Remote Sensing, vol. 10, no. 5, p. 789, 2018.
[8] M. S. K. McFeeters, "The use of the Normalized Difference Water Index (NDWI) in the delineation of open water features," International Journal of Remote Sensing, vol. 17, no. 7, pp. 1425–1432, 1996.
[9] S. Aryal, S. Shrestha, and A. M. Tuladhar, "Assessment of landslide susceptibility using satellite imagery and geospatial analysis in Nepal," Landslides, vol. 17, no. 8, pp. 1927–1941, 2020.
[10] M. A. H. Bhuiyan, M. A. Islam, and M. A. Bari, "Evaluation of Digital Elevation Models for flood inundation modeling in flat deltaic plains: A case study in Bangladesh," Environmental Monitoring and Assessment, vol. 186, no. 8, pp. 5361–5376, 2014.
[11] W. R. Azizah and A. W. Wijayanto, "Design and implementation of an interactive visualization dashboard for monitoring flood vulnerability and mapping," in Proc. Int. Conf. on Data Science and Official Statistics, 2023.
[12] D. W. Triscowati, B. Sartono, A. Kurnia, D. D. Domiri, and A. W. Wijayanto, "Multitemporal remote sensing data for classification of food crops plant phase using supervised random forest," in Sixth Geoinformation Science Symposium, p. 10, 2019, doi: 10.1117/12.2547216.
[13] T. D. T. Saadi and A. W. Wijayanto, "Machine learning applied to Sentinel-2 and Landsat-8 multispectral and medium-resolution satellite imagery for the detection of rice production areas in Nganjuk, East Java, Indonesia," International Journal of Remote Sensing and Earth Sciences, vol. 18, no. 1, 2021.
[14] P. Tripathy and T. Malladi, "Global Flood Mapper: A novel Google Earth Engine application for rapid flood mapping using Sentinel-1 SAR," Natural Hazards, pp. 1341–1363, 2022. [Online]. Available: https://pratyush-tripathy.users.earthengine.app/view/global-flood-mapper-advanced
[15] Badan Nasional Penanggulangan Bencana (BNPB), Risiko bencana banjir di Indonesia, 2024. [Online]. Available: https://inarisk.bnpb.go.id/pdf/INDONESIA/risiko_banjir_INDONESIA.pdf. [Accessed: Apr. 2, 2024].
[16] Badan Pusat Statistik, Citizenship ethnicity, religion, language 2010, 2010. [Online]. Available: demografi.bps.go.id. [Archived: Jul. 12, 2017; Accessed: Apr. 23, 2024].
[17] A. Pindarwati and A. W. Wijayanto, "Measuring performance level of smart transportation system in big cities of Indonesia comparative study: Jakarta, Bandung, Medan, Surabaya, and Makassar," in Proc. 2015 Int. Conf. on Information Technology Systems and Innovation (ICITSI), pp. 1–6, 2015.
[18] S. R. Putri, A. W. Wijayanto, and S. Pramana, "Multi-source satellite imagery and point of interest data for poverty mapping in East Java, Indonesia: Machine learning and deep learning approaches," Remote Sensing Applications: Society and Environment, vol. 29, p. 100889, 2023.
[19] Y. C. Putra and A. W. Wijayanto, "Automatic detection and counting of oil palm trees using remote sensing and object-based deep learning," Remote Sensing Applications: Society and Environment, vol. 29, p. 100914, 2023.